JOURNAL OF AIRCRAFT
Vol. 38, No. 2, March–April 2001

Flutter Prediction from Flight Flutter Test Data

G. Dimitriadis* and J. E. Cooper†
University of Manchester, Manchester, England M13 9PL, United Kingdom

The most common approach to flight flutter testing is to track estimated modal damping ratios of an aircraft over a number of flight conditions. These damping trends are then extrapolated to predict whether it is safe to move to the next test point and also to determine the flutter speed. In the quest for more reliable and efficient flight flutter testing procedures, a number of alternative data analysis methods have been proposed. Five of these approaches are compared on two simulated aeroelastic models. The comparison is based on both the accuracy of prediction and the efficiency of each method. It is found that, for simple aeroelastic systems, the Nissim and Gilyard method (Nissim, E., and Gilyard, G. B., "Method for Experimental Determination of Flutter Speed by Parameter Identification," AIAA Paper 89-1324, 1989) yields the best flutter predictions and is also the least computationally expensive approach. However, for larger systems, simpler approaches such as the damping fit and envelope function methods are found to be most reliable.

Nomenclature

A_i	=	polynomial coefficients in characteristic equation, flutter margin method (FM)
$\boldsymbol{A}_i$	=	aerodynamic matrix coefficients, Nissim and Gilyard method (NG)
$a(m)$	=	moving average (MA) coefficients, autoregressive moving average method (ARMA)
$b(m)$	=	autoregressive (AR) coefficients, ARMA
$\boldsymbol{C}_s$	=	structural damping matrix, NG
$\bar{\boldsymbol{C}}$	=	damping matrix, NG
env(t)	=	decay envelope or envelope function, envelope function method
F	=	flutter margin, FM
$\bar{\boldsymbol{F}}$	=	forcing vector, NG
$F^{\pm}(l)$, $G(1)$, $G(-1)$	=	Jury stability criteria, ARMA
$g(t)$	=	forcing function, NG
J	=	model order, ARMA
$\boldsymbol{K}_s$	=	structural stiffness matrix, NG
$\bar{\boldsymbol{K}}$	=	stiffness matrix, NG
$\bar{\boldsymbol{M}}$	=	mass matrix, NG
m	=	number of degrees of freedom, NG
n_f	=	number of points used in identification, NG
q	=	dynamic pressure, FM
$\boldsymbol{q}$	=	generalized coordinates, NG
S	=	shape function, envelope function method
$\bar{t}$	=	time centroid of decay envelope, envelope function method
$u(i)$	=	discrete values of input, ARMA
V_f	=	flutter velocity
V_∞	=	freestream velocity, NG
$y(i)$	=	discrete values of output, ARMA
$y(t)$	=	impulse response, envelope function method
$y_H(t)$	=	Hilbert transform of the impulse response, envelope function method
β	=	reference length, NG
β_i	=	real part of ith eigenvalue, FM
ζ	=	damping ratio, ARMA
λ_i	=	ith eigenvalue, FM
ρ	=	density of air, NG
ω	=	natural frequency, ARMA
ω_i	=	imaginary part of ith eigenvalue, FM

Received 20 May 1999; revision received 15 September 2000; accepted for publication 15 November 2000.

*Lecturer, Aerospace Engineering, Oxford Road.
†Senior Lecturer, Aerospace Engineering, Oxford Road. Member AIAA.

Introduction

DURING the design stage of a new aircraft, the aeroelastic behavior is estimated by producing detailed mathematical and aeroelastic wind-tunnel models. The critical phenomenon is flutter, a violent unstable oscillation, which must be avoided throughout the flight envelope. Airworthiness regulations require that stability throughout the required flight regime is demonstrated by tests of the actual flying aircraft, commonly termed flight flutter tests. Flight flutter tests consist of flying an aircraft at a range of subcritical air speeds while applying some form of excitation to the structure. The response of the structure is measured at a number of measurement stations, and the data is curve fitted to determine the stability at the current flight speed and predict whether it is safe to proceed to the next test point. Of interest is the speed at which flutter is predicted. This process is repeated at numerous flight conditions until the envelope is cleared. In practice, the most common response data analysis procedure is to estimate the damping present in the aircraft response and to track its variation with air speed.

Even in the days of high-speed computers and sophisticated data measurement and analysis tools, flutter testing remains as much an art as a science. Subcritical damping data cannot always be safely extrapolated to obtain an accurate prediction for the flutter velocity. Nonlinearities in the control system or in the aerodynamics and structure of an aircraft can critically affect the aeroelastic behavior. Finally, the aeroelastic stability can change from positive to negative with an increase in air speed of only a few knots, and the whole procedure is very dangerous and time consuming.

There are various methods to predict the flutter speed using flight flutter test data. The purpose of this paper is to examine and compare a number of the approaches that are used in industry and appear in the literature. This comparison has not been attempted before to the authors' knowledge. Both the efficiency and quality of the predictions obtained by the methods are compared using simulated systems to provide a comprehensive overview of contemporary flutter prediction procedures. A more accurate and efficient flutter prediction would decrease the time taken for flight flutter testing as well as increase safety.

Flutter Prediction Methods

Damping Ratio Variation with Air Speed

Traditionally, the most widely used indicators of the stability of an aeroelastic system are the modal dampings and their variation with freestream velocity. At flutter, the damping in at least one of the modes is zero, thus causing self-excited oscillations. Beyond this speed, the system becomes unstable. In the typical flight flutter test, the damping ratios for all of the significant modes are evaluated at a number of subcritical air speeds using system identification

methods. The damping ratio trends are then curve fitted by a polynomial, or by hand, and extrapolated to estimate the flutter velocity and to examine the stability at the next proposed flight test.

There are numerous system identification methods, both in the time and the frequency domain, that allow the calculation of the modal parameters of a vibrating system.[1] Here, a version of the rational fraction polynomial method[2] is used. Obviously, the accuracy of predicting the flutter speed depends on how well the damping ratios are estimated.

Flutter Margin Method

The flutter margin method (FM) was first presented in Ref. 3. The basis of the approach is the quest for a more fundamental stability criterion than just tracking the damping present in the system. In its original form, the approach only covers binary flutter; however, in Ref. 4 an extension of the technique to trinary flutter is presented.

The FM employs the Routh stability criterion.[5] For a two-degree-of-freedom system, for which the characteristic equation is a quartic of the form

$$\lambda^4 + A_3\lambda^3 + A_2\lambda^2 + A_1\lambda + A_0 = 0 \tag{1}$$

the Routh stability criterion reduces to

$$[A_2(A_1/A_3) - (A_1/A_3)^2 - A_0] > 0 \tag{2}$$

Hence, for a two-degree-of-freedom system, there is a quantity described by Eq. (2) that has to be positive for the system to be stable and becomes zero when instability is reached. This quantity is termed the flutter margin and is given by (in slightly modified form)

$$F = \left[\left(\frac{\omega_2^2 - \omega_1^2}{2}\right) + \left(\frac{\beta_2^2 - \beta_1^2}{2}\right)\right]^2 + 4\beta_1\beta_2\left[\left(\frac{\omega_2^2 + \omega_1^2}{2}\right) + 2\left(\frac{\beta_2 + \beta_1}{2}\right)^2\right] - \left[\left(\frac{\beta_2 - \beta_1}{\beta_2 + \beta_1}\right)\left(\frac{\omega_2^2 - \omega_1^2}{2}\right) + \left(\frac{\beta_2 + \beta_1}{2}\right)^2\right]^2 \tag{3}$$

which is obtained from Eq. (3), after substituting for the two sets of complex conjugate eigenvalues, $\lambda_1, \ldots, \lambda_4$, such that

$$\lambda_{1,2} = \beta_1 \pm i\omega_1, \qquad \lambda_{3,4} = \beta_2 \pm i\omega_2$$

The application of the method is quite straightforward. For a two-degree-of-freedom system, the response to a known input at a particular (subcritical) air speed is recorded and the eigenvalues of the system are calculated.[1] These are then used to compute the flutter margin. Where some further derivation[3] is used, it can be shown that the flutter margin is a quadratic function of the dynamic pressure, that is,

$$F = B_2q^2 + B_1q + B_0 \tag{4}$$

where B_0, B_1, and B_2 are coefficients to be evaluated. Hence, if the flutter margin is known at three different air speeds, it can be fitted by a second-order polynomial and subsequently extrapolated. Flutter occurs when $F = 0$. In practice, to counteract the effects of experimental uncertainty, the flutter margin is estimated at a wider range of subcritical air speeds and then fitted in a least-squares sense.

That the flutter margin is derived for a two-degree-of-freedom system does not imply that the method cannot be used with larger systems. In fact, the flutter mechanism is often dependent on two modes only. If it is known beforehand which two modes will cause flutter, the FM can be applied successfully; otherwise, all possible pairs of modes must be examined.

Some experimental evaluation of the method suggests that using a quadratic fit of the flutter margin can yield results that are very sensitive to errors or uncertainty in the experimental data.[6] An alternative is to use linear extrapolation, again in a least-squares sense.

Envelope Function

The envelope function[7] was originally proposed as a tool to provide an assessment of overall stability to complement standard analysis. However, it has since been used in practice to provide flight flutter clearance of the ALTOS high-altitude research aircraft.

The basis of the method is that the impulse response of any stable damped system is decaying, with the shape of the decay in the time domain being described by the decay envelope. As the damping in a given aeroelastic system decreases, the decay envelope grows wider, eventually becoming a rectangle as the damping becomes zero. When the position of the centroid of the decay envelope and the way that it shifts on the time axis as the damping decreases are evaluated, it is possible to assess the stability of the system.

For an aeroelastic system with impulse response $y(t)$, the decay envelope, or envelope function, is given by

$$\text{env}(t) = \sqrt{y(t)^2 + y_H(t)^2} \tag{5}$$

where $y_H(t)$ is the Hilbert transform of the impulse response, defined as

$$y_H(t) = F^{-1}\{\text{Im}[Y(\omega)]\} - j\text{Re}[Y(\omega)] \tag{6}$$

where $Y(\omega)$ is the Fourier transform of $y(t)$ and Im and Re are imaginary and real part, respectively. The time centroid of the decay envelope is given by

$$\bar{t} = \frac{\int_0^{t_{\max}} \text{env}(t)t\,\mathrm{d}t}{\int_0^{t_{\max}} \text{env}(t)\,\mathrm{d}t} \tag{7}$$

The upper limit of integration, $t_{\max}$, serves to define the rectangle within which the integration takes place. For a single-degree-of-freedom system, when the damping is zero, the time centroid lies at $t = t_{\max}/2$. For a multi-degree-of-freedom system, it is suggested that $t \approx t_{\max}/2$ is an adequate approximation for the position of the time centroid.[7]

Because $\bar{t}$ tends to increase as the damping drops, its inverse is usually employed as the significant shape parameter, that is,

$$S = 1/\bar{t} \tag{8}$$

in which case the value of S at the flutter condition is $S = 2/t_{\max}$ for a single-degree-of-freedom system. For multi-degree-of-freedom systems $S \approx 2/t_{\max}$.

The envelope function flutter testing procedure is to evaluate S at a number of subcritical air speeds. The variation of S with air speed is then curve fitted using a polynomial, as with the damping method, and extrapolated to the point where $S = 2/t_{\max}$, thus yielding the flutter velocity.

The impulse response of an aeroelastic system may be obtained in two ways: 1) direct measurement of the aircraft response to impulsive excitation, for example, stick jerk, and 2) application of other excitation functions, for example, white noise, chirp. The Fourier transforms of the response and excitation are then divided to yield the frequency response function (FRF). The impulse response is obtained as the inverse Fourier transform of the FRF.

In the present implementation, the second approach was chosen. The disadvantage of the first technique is that, in practice, it is impossible to apply a perfect impulse to a system as complex as an aircraft; hence, the measured response may not be close enough to the impulse response. The second approach also allows the smoothing of some of the measurement noise by careful choice of the Fourier transform window. Additionally, the impulse responses can be exponentially weighted[8] to improve the noise-to-signal ratio at the tail end of the response.

Nissim and Gilyard Method

The two methods already described deal with attempting to evaluate the stability of a given aeroelastic system and, hence, the flutter velocity. The Nissim and Gilyard method (NG),[9] which is an extension to a technique developed by Skingle et al.,[10] adopts a different approach by attempting to identify the whole system, including its aerodynamic variation with freestream air speed by estimating its equations of motion. Then, the identified system can be solved for different velocities to obtain the flutter speed.

The equations of motion for a forced aeroelastic system are

$$\bar{\boldsymbol{M}}\ddot{\boldsymbol{q}} + \bar{\boldsymbol{C}}\dot{\boldsymbol{q}} + \bar{\boldsymbol{K}}\boldsymbol{q} = \bar{\boldsymbol{F}}g(t) \tag{9}$$

If Eq. (9) is transposed to the frequency domain and premultiplied by $\bar{\boldsymbol{M}}^{-1}$, the equations of motion become

$$\{-\boldsymbol{I}\omega^2 + \boldsymbol{C}\jmath\omega + \boldsymbol{K}\}\boldsymbol{q}(\omega) = \boldsymbol{F}g(\omega) \tag{10}$$

where

$$\boldsymbol{C} = \bar{\boldsymbol{M}}^{-1}\bar{\boldsymbol{C}}, \qquad \boldsymbol{K} = \bar{\boldsymbol{M}}^{-1}\bar{\boldsymbol{K}}, \qquad \boldsymbol{F} = \bar{\boldsymbol{M}}^{-1}\bar{\boldsymbol{F}}$$

and multiplication by $\jmath\omega$ denotes differentiation. Divide both sides of Eq. (10) by $g(\omega)$ and rearrange

$$\boldsymbol{C}\jmath\omega\boldsymbol{H}_q(\omega) + \boldsymbol{K}\boldsymbol{H}_q(\omega) - \boldsymbol{F} = \boldsymbol{I}\omega^2\boldsymbol{H}_q(\omega) \tag{11}$$

where $\boldsymbol{H}_q(\omega) = \boldsymbol{q}(\omega)/g(\omega)$. For an m-degree-of-freedom system, Eq. (11) can be rearranged and expanded as

$$\begin{pmatrix} H_{q_1}(\omega_1) & \dots & H_{q_m}(\omega_1) & \jmath\omega_1 H_{q_1}(\omega_1) & \dots & \jmath\omega_1 H_{q_m}(\omega_1) & -1 \\ H_{q_1}(\omega_2) & \dots & H_{q_m}(\omega_2) & \jmath\omega_2 H_{q_1}(\omega_2) & \dots & \jmath\omega_2 H_{q_m}(\omega_2) & -1 \\ \vdots & \vdots & \vdots & \vdots & \vdots & \vdots & \vdots \\ H_{q_1}(\omega_{n_f}) & \dots & H_{q_m}(\omega_{n_f}) & \jmath\omega_{n_f} H_{q_1}(\omega_{n_f}) & \dots & \jmath\omega_{n_f} H_{q_m}(\omega_{n_f}) & -1 \end{pmatrix} \begin{pmatrix} \boldsymbol{K}^T \\ \boldsymbol{C}^T \\ \boldsymbol{F}^T \end{pmatrix} = \begin{pmatrix} \omega_1^2 H_{q_1}(\omega_1) & \dots & \omega_1^2 H_{q_m}(\omega_1) \\ \omega_2^2 H_{q_1}(\omega_2) & \dots & \omega_2^2 H_{q_m}(\omega_2) \\ \vdots & \vdots & \vdots \\ \omega_{n_f}^2 H_{q_1}(\omega_{n_f}) & \dots & \omega_{n_f}^2 H_{q_m}(\omega_{n_f}) \end{pmatrix} \tag{12}$$

Equation (12) is of the form

$$\boldsymbol{T}\boldsymbol{X} = \boldsymbol{B} \tag{13}$$

where $\boldsymbol{X}$ is to be evaluated in a least-squares sense. Strictly speaking, n_f only needs to be equal to m for a successful identification; however, to counteract the effect of noise in the responses, usually $n_f > m$ and the equation is solved in a least-squares sense. For increased accuracy, multiple forcing vectors can be applied to the system. This is particularly relevant to the case where the responses include a high level of noise.

To obtain an identified model of the system at all air speeds, a second identification needs to take place at a different freestream velocity. According to Ref. 11, the unsteady aerodynamic matrix $\boldsymbol{Q}(\jmath\omega)$ for an aeroelastic system is given by

$$\boldsymbol{Q}(\jmath\omega) = \frac{1}{2}\rho V_\infty^2 \left[\bar{\boldsymbol{A}}_0 + \bar{\boldsymbol{A}}_1 \jmath\omega \left(\frac{b}{V_\infty}\right) + \bar{\boldsymbol{A}}_2 (\jmath\omega)^2 \left(\frac{b}{V_\infty}\right)^2 + \left(\frac{V_\infty}{b}\right) \sum_{n=1}^{n_L} \frac{\bar{\boldsymbol{A}}_{(n+2)}}{\jmath\omega + (V_\infty/b)b_n} \right] \tag{14}$$

where n_L depends on the desired accuracy but is usually no more than four, b is a reference length, and $\bar{\boldsymbol{A}}_0, \dots, \bar{\boldsymbol{A}}_{n_L}$ are matrix coefficients. For a quasi-steady aerodynamic representation, the lag terms are ignored leading to

$$\boldsymbol{Q}(\jmath\omega) = \tfrac{1}{2}\rho V_\infty^2 \boldsymbol{A}_0 + \tfrac{1}{2}\rho V_\infty \boldsymbol{A}_1 \jmath\omega \tag{15}$$

where $\boldsymbol{A}_i = b^i \bar{\boldsymbol{A}}_i$ for $i = 1, 2$; $\boldsymbol{A}_0$ are aerodynamic stiffness terms; and $\boldsymbol{A}_1$ are aerodynamic damping terms. Terms $\boldsymbol{A}_2$, representing aerodynamic inertia terms, have also been neglected because they are usually very small compared to structural inertia terms. In other words, matrices $\boldsymbol{C}$ and $\boldsymbol{K}$ in Eq. (12) can be broken down into structural and aerodynamic part, that is,

$$\boldsymbol{C} = \boldsymbol{C}_s + \tfrac{1}{2}\rho V_\infty \boldsymbol{A}_1, \qquad \boldsymbol{K} = \boldsymbol{K}_s + \tfrac{1}{2}\rho V_\infty^2 \boldsymbol{A}_0 \tag{16}$$

with subscript s denoting structural terms. If the identification process described earlier is repeated at two distinct velocities, then the structural and aerodynamic matrices can be evaluated separately and the behavior of the system at any air speed can be predicted either by integrating the equations of motion or by calculating the system's eigenvalues. Finally, the flutter speed can be obtained by means of a suitable iterative calculation, for example, evaluating the system damping at increasing speeds until flutter is reached.

It should be noted that the NG requires modal responses to work. Consequently, if only physical coordinates $\boldsymbol{z}$ are available, then the modal matrix Φ should be evaluated and used to obtain the modal coordinates from

$$\boldsymbol{z} = \Phi\boldsymbol{q} \tag{17}$$

Autoregressive Moving Average-Based Method

The equations of motion of a dynamic system can be expressed as a sum of the regressive response terms equal to the value of the regressive forcing term. This is the basis of the representation of dynamical systems by autoregressive moving-average (ARMA) models, where the AR part denotes the terms containing the response y and the MA part denotes the white noise excitation terms u.

The general form of an ARMA is[12]

$$\sum_{m=0}^{2J} b(m)y(i+m) = \sum_{m=0}^{2J-1} a(m)u(i+m) \tag{18}$$

The order of the model, J, can be equal to the number of modes of the system to be modeled but, in the presence of experimental noise, it is usually taken to be greater than the number of modes.

To identify a given dynamic system, the ARMA equation is applied to a set of single input/single output sampled data. The unknown coefficients, a, b, and J are evaluated using a parameter estimation algorithm, the simplest of which is the least-squares procedure. This evaluation can be simplified by dividing the ARMA equation throughout by $b(2J)$, so that the leading AR coefficient is always unity.

If Eq. (18) is evaluated at instances $i = 1, \dots, k$, then the coefficients can be obtained using

$$\begin{pmatrix} y(2J) & \dots & y(1) & u(2J) & \dots & u(1) \\ y(2J+1) & \dots & y(2) & u(2J+1) & \dots & u(2) \\ \vdots & \vdots & & \vdots & \vdots & \\ y(2J+k-1) & \dots & y(k) & u(2J+k-1) & \dots & u(k) \end{pmatrix} \times \begin{Bmatrix} b(2J-1) \\ \vdots \\ b(0) \\ a(2J-1) \\ \vdots \\ a(0) \end{Bmatrix} = -\begin{Bmatrix} y(2J+1) \\ y(2J+2) \\ \vdots \\ y(2J+k) \end{Bmatrix} \tag{19}$$

This matrix equation can be solved using any number of schemes, such as those described in Refs. 13 and 14. The eigenvalues of the system can be obtained by forming the characteristic polynomial

$$G(\mu) = \mu^{2J} + b(2J-1)\mu^{2J-1} + \cdots + b(1)\mu + b(0) = 0 \quad (20)$$

and, subsequently, evaluating its roots

$$\mu_{1,2} = \exp\left[\left(-\zeta\omega \pm j\omega\sqrt{1-\zeta^2}\right)\Delta t\right] \quad (21)$$

The ARMA method, as described up to now is a system identification technique. Matsuzaki et al.[12] suggest a procedure for using an ARMA representation of an aeroelastic system as a means of predicting the flutter velocity. The basis of the approach is the Jury determinant method for evaluating the stability of a discrete-time system, which is very similar to the Routh–Hurwitz criterion for continuous-time systems (used in conjunction with the FM). The Jury stability criterion applies to the characteristic polynomial, Eq. (20), such that the system is stable if

$$G(1) > 0, \qquad G(-1) > 0 \quad (22)$$

and for $l = 1, 3, \ldots, 2J-1$,

$$F^{\pm}(l) = \left|X_l^* \pm Y_l^*\right| > 0 \quad (23)$$

where X_{2J-1}^* and Y_{2J-1}^* are $(2J-1)\times(2J-1)$ matrices, given by

$$X_{2J-1}^* = \begin{pmatrix} b(2J) & b(2J-1) & \ldots & \ldots & b(3) & b(2) \\ 0 & b(2J) & b(2J-1) & \ldots & b(4) & b(3) \\ 0 & 0 & b(2J) & \ldots & b(5) & b(4) \\ \vdots & & \vdots & & \vdots & \\ 0 & \ldots & \ldots & \ldots & \ldots & b(2J) \end{pmatrix} \quad (24)$$

$$Y_{2J-1}^* = \begin{pmatrix} b(2J-2) & b(2J-3) & \ldots & \ldots & b(1) & b(0) \\ b(2J-3) & b(2J-4) & \ldots & \ldots & b(0) & 0 \\ b(2J-4) & b(2J-5) & \ldots & b(0) & 0 & 0 \\ \vdots & & & \vdots & & \\ b(0) & 0 & \ldots & \ldots & \ldots & 0 \end{pmatrix} \quad (25)$$

Consequently, the flutter condition is defined as the first air speed at which any of the criteria $G(1)$, $G(-1)$, and $F^{\pm}(l)$ becomes zero. Hence, the system can be identified at a range of velocities, and the values of the criteria plotted against air speed and then curve fitted by a polynomial to yield the points were they intersect the velocity axis and, hence, the flutter velocities. This particular implementation of the Jury stability criterion is disadvantageous compared to the FM in that the criteria do not vary in a predictable manner with velocity. Instead, if polynomial fitting is attempted, the order will not be known, as with the damping fit and envelope methods.

Preliminary Validation of the Methods

The methods were applied to two simulated aeroelastic models, one of them modeling a simple, three-degree-of-freedom, rectangular wing with control surface, referred to as the Hancock model (see Ref. 15) and the other modeling a four-engined civil transport,[7] referred to as the Sim-2 model. The Hancock model was chosen to demonstrate the methods on the most simplistic aeroelastic model possible. The Sim-2 model was chosen because it is a multimodal, industrially validated model and is characteristic of a number of commercial aircraft. Nevertheless, in both cases the flutter mechanism is essentially binary. Figures 1 and 2 show the variation of natural frequencies and damping ratios for both models. In the case of the Sim-2 model, only some representative modes are plotted. The flutter speeds of the two models were 44.07 m/s for the Hancock model and 398 kn for the Sim-2 model (5000 ft).

With both models, and for all of the methods, the excitation waveforms used were frequency sweeps, sweeping through all of the natural frequencies of the models so as to excite all modes. The excitation forces were applied through control surfaces and were symmetric. Additionally, all responses were contaminated by 5% rms simulated noise to approximate the effects of experimental uncertainty. Each method was tested in a variety of velocity ranges, as shown in Tables 1 and 2 for the Hancock and Sim-2 models, respectively. In each of the ranges, a number of tests were performed at increments of 7% of the true flutter speed. Results for the NG are not presented for the Sim-2 model, for reasons that will be explained later.

Noted that the validation of the methods presented here is specific to the particular models and implementations chosen.

Damping Fit Method

Preliminary tests of the method showed that curve fits by a range of polynomial orders (between 3 and 8) can give the optimal flutter

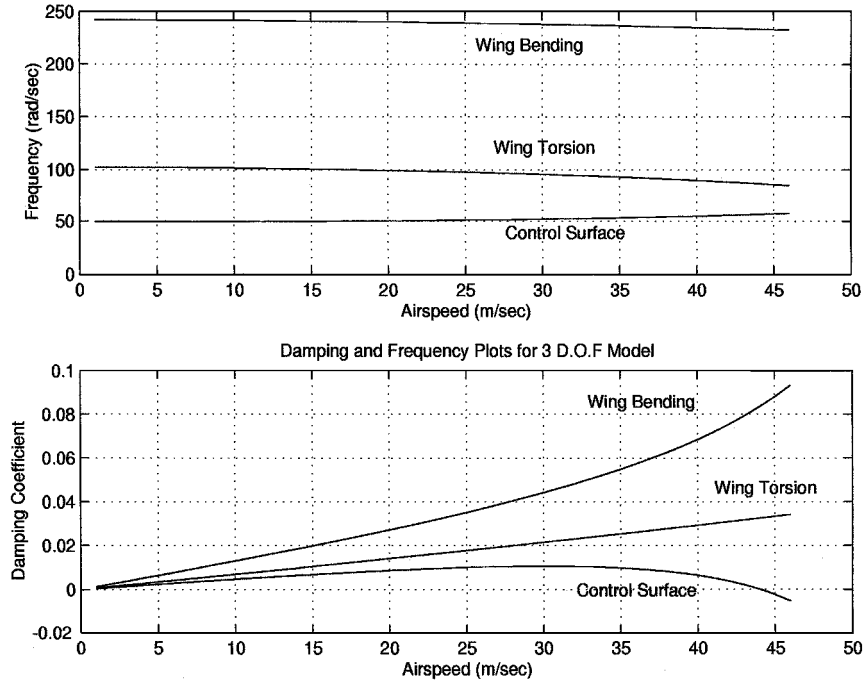

Fig. 1 Variation of natural frequencies and dampings with air speed, Hancock model.

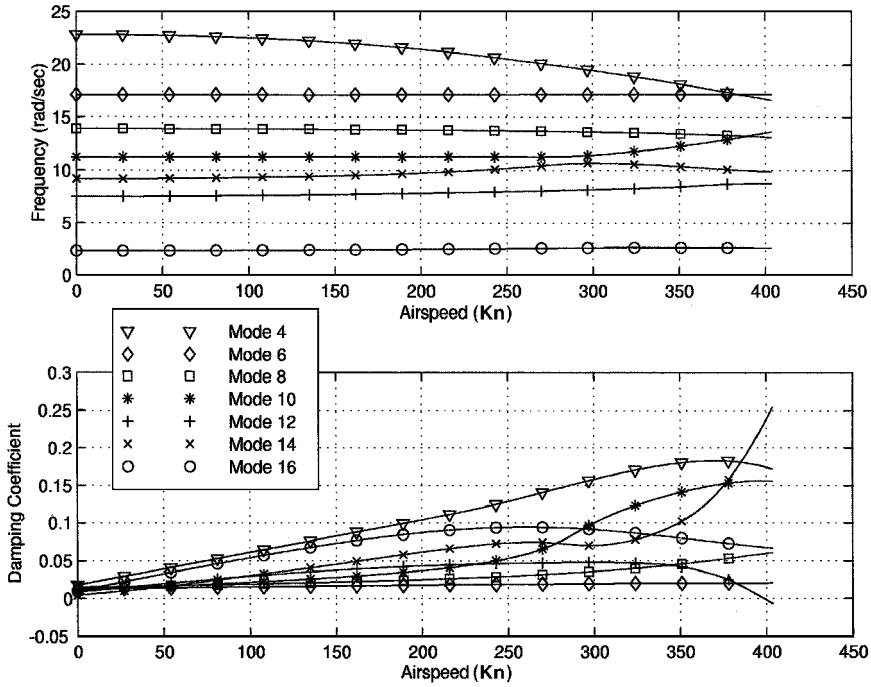

Fig. 2 Variation of natural frequencies and dampings with air speed, Sim-2 model.

Table 1 Modulus of errors in flutter estimates, Hancock model

Velocity range (% of flutter speed)	Damping fit, %	FM, %	Envelope, %	NG, %	ARMAX, %
23–43	14.4	6.8	13.0	2.5	46.2
23–57	5.1	3.9	2.1	4.7	17.5
23–70	9.1	2.5	0.6	1.3	21.0
23–84	0.1	1.1	4.8	0.1	15.4
23–98	0.5	0.3	0.1	0.1	0.3
45–66	17.5	1.3	6.9	0.8	23.6
45–79	0.9	1.7	1.9	0.7	8.7
45–93	0.1	0.1	0.3	0.2	1.6
68–88	0.2	0.8	0.4	0.7	6.1

Table 2 Modulus of errors in flutter estimates, Sim-2 model

Velocity range (% of flutter speed)	damping fit, %	FM, %	Envelope, %	ARMAX, %
23–43	28.4	——	5.5	53.3
23–57	17.0	18.8	35.1	32.9
23–70	9.2	15.5	16.2	6.5
23–84	4.6	3.8	2.5	8.7
23–98	0.3	0.8	0.7	1.0
45–66	2.8	20.8	9.4	12.1
45–79	2.3	5.5	6.0	8.7
45–93	0.5	——	1.3	2.2
68–88	2.9	——	0.5	2.0

predictions. Additionally, changing the polynomial order by one can give wildly inaccurate results. In general, orders between three and six are the most suitable choices; however, flutter predictions in Tables 1 and 2 were out by up to 17.5% of the true flutter speed for the Hancock model and 28.4% for the Sim-2 model. Furthermore, if too high an order is used (typically above 10, depending on how many points are fitted), the matrix used for the polynomial fit becomes rank deficient, and the fit itself fails completely.

Damping trends tend to be relatively smooth and no more than quartic in shape even when hard flutter is encountered. In actual fact, no case was encountered where the use of polynomial orders higher than six was needed. However, this is by no means a general result.

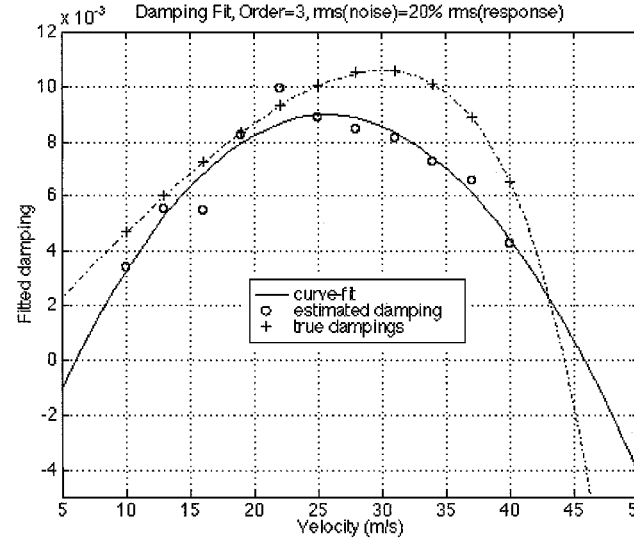

Fig. 3 Flutter prediction using damping fit; 20% rms noise.

Because, in practice, the flutter speed is not known in advance, it is impossible to predict which order of fit will give the best estimate.

The sensitivity of the method to noise is governed by the sensitivity of the rational fraction polynomial (RFP) procedure. The deteriorating quality of the latter with increasing levels of noise affects the flutter prediction negatively, as is seen in Fig. 3, where a flutter prediction is shown for results with 20% rms noise. In Fig. 3, the circles are estimated damping ratio data, the solid curve is the best-case polynomial fit of the estimated damping data, the crosses are theoretical damping data, and the dashed curve the best-case polynomial fit of the theoretical damping ratio data (obtained from the equations of motion). A comparison between the latter and the best-case fit of the estimated damping ratios shows that the flutter speed has been overestimated by quite a margin (4.4%) and also that the estimated subcritical behavior of the damping curve is wrong.

FM

As mentioned earlier, successful application of the FM to a multi-degree-of-freedom (DOF) aeroelastic system depends on the

knowledge of the flutter mechanism, that is, which two modes will combine to cause flutter. When the technique is applied to these two modes, a representative system is analyzed. Note that flutter margins calculated from any combination of modes containing the mode that becomes unstable at flutter will become zero at the flutter velocity. In Ref. 16 it is shown that Eq. (3) can be rewritten as

$$F = \left[1 - \left(\frac{\beta_2 - \beta_1}{\beta_2 + \beta_1}\right)^2\right]\left\{\left(\frac{\omega_2^2 - \omega_1^2}{2}\right)^2 + (\beta_1 + \beta_2)^2\left[\left(\frac{\omega_2^2 + \omega_1^2}{2}\right) + \left(\frac{\beta_2 + \beta_1}{2}\right)^2\right]\right\} \tag{26}$$

It is obvious that, if either β_1 or β_2 become zero, then

$$\left[1 - \left(\frac{\beta_2 - \beta_1}{\beta_2 + \beta_1}\right)^2\right] = 0 \tag{27}$$

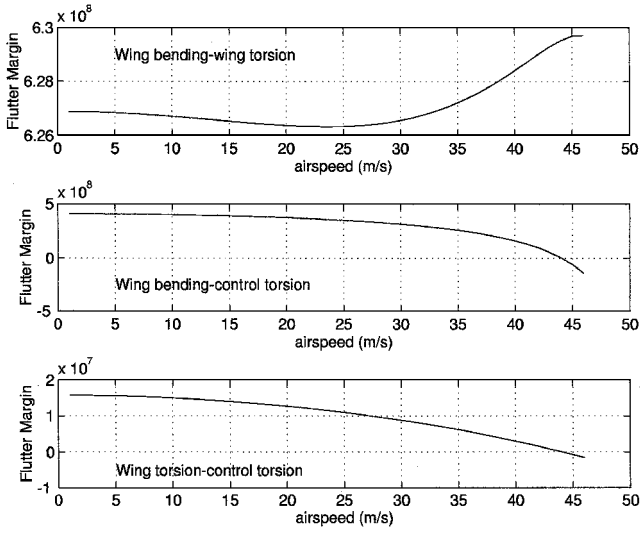

Fig. 4 Flutter margin variation for the three possible flutter mechanisms, Hancock model.

and F also becomes zero. This phenomenon is shown in Fig. 4 for the Hancock model, whose flutter mechanism includes the wing torsion and control surface torsion modes, the damping of the control surface torsion mode becoming zero at flutter. Figure 4 shows flutter margins calculated for all three combinations of modes. In the wing bending–wing torsion case, the flutter margin never becomes zero. In the other two cases, which contain the control surface torsion mode, the flutter margin becomes zero at flutter. This phenomenon is because any system formed of two modes from another system, one of which is unstable, will also be unstable. However, Fig. 4 shows that the variation of the flutter margin with air speed for the wing bending-control surface torsion case is not quadratic. In other words, a number of spurious flutter margins, or parameters indicating the stability of a multi-DOF system, can be formed using the FM but these parameters will not be the flutter margin, as defined by Zimmerman and Weissenburger.[3] Only if the actual flutter mechanism is used will the flutter margin be obtained.

The application of the FM to the Sim-2 model was not as straightforward as in the Hancock case. The Sim-2 model contains 23 modes, of which mode 12 becomes unstable at flutter. The flutter mechanism consists of mode 12 and mode 4. The flutter margin variation with speed for the actual flutter mechanism is shown in Fig. 5. Notice that the variation is not exactly quadratic because such a variation can only be obtained for systems with no structural damping,[4] whereas the Sim-2 model has nonzero damping at zero speed, which is equivalent to structural damping. Unfortunately, mode 4 is highly, damped with respect to most of the other modes and, hence, does not feature prominently in any of the FRFs, even at speeds which are low compared to the flutter speed. Because, for this work, the eigenvalues were obtained using a frequency-domain method, the eigenvalue of mode 4 could not always be obtained. The FM results of Table 2 have gaps were the eigenvalues of the modes were not obtained. As a consequence, an alternative approach was used for the simulated flutter tests described later. The FM was applied to the combination of modes 12 and 3, the latter being a prominent mode in the FRFs. Equation (3) was applied to these two modes yielding a spurious flutter margin that did not vary quadratically and had to be curve fitted by higher-order polynomials. Nevertheless, because the spurious flutter margin became zero at flutter, it served as a stability parameter. The combination of modes 12 and 3 was chosen after all of the other possible combinations were tested.

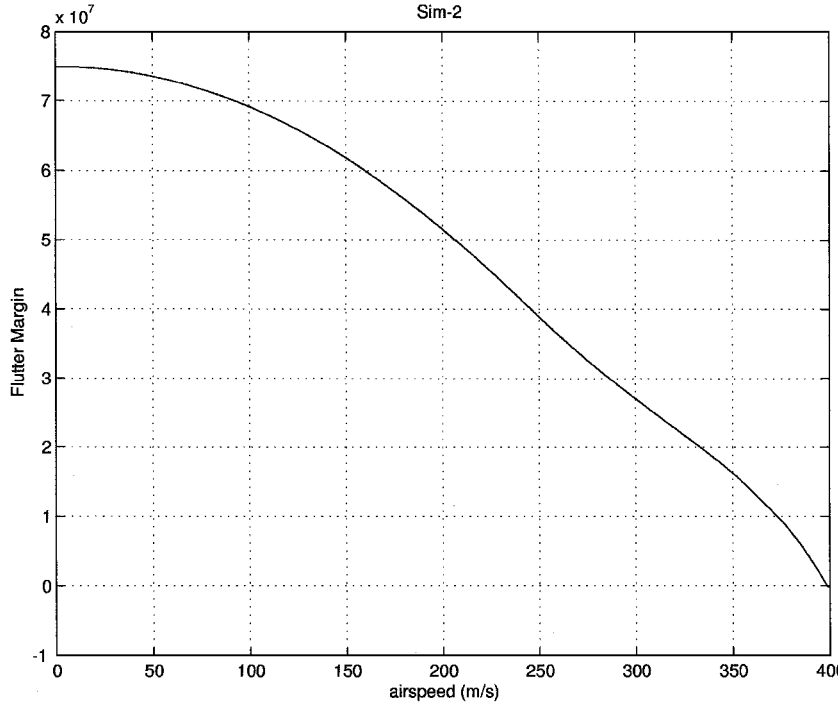

Fig. 5 True flutter margin variation with air speed, Sim-2 model.

As with the damping fit approach, the FM's sensitivity to noise depends on that of the RFP. It is at these conditions that the authors of Ref. 6 suggest a linear fit of the flutter margin gives better estimates for the flutter velocity. However, Fig. 6 shows that this latter approach would provide worse results than the normal quadratic fit on the Hancock model.

Envelope Function Method

The main considerations in the successful application of the envelope function method are the number and velocities of subcritical tests, the order of the polynomial fit of the decay envelope centroid, and the values of t_{max}, and noise. When testing a multi-DOF system, a number of responses can be measured, all of which will yield an envelope function and a shape parameter at each air speed, as seen in Fig. 7 for the Hancock model, where the shape parameter variation with air speed for each DOF is plotted. Hence, the shape parameters from every measured response can be curve fitted to yield an estimate for the flutter velocity.

The advantage of applying the method to a large system with many measurement positions, such as the Sim-2 model, is that responses from all of these positions can be used to calculate shape parameters. Even if some of the responses overshoot the decay envelope flutter criterion because of measurement error, on average the criterion is satisfied. This statement can be verified by Fig. 8, which shows a plot of shape parameters from each measuring position in the case where the impulse responses were corrupted with 10% rms noise. Hence, the envelope function flutter prediction procedure can be modified to include curve fitting of the shape parameters of all of the measured impulse responses (17 for the Sim-2 model).

The presence of noise in the system responses causes a deterioration in the quality of the estimated impulse responses. This deterioration, in turn, causes significant scatter in the results for the position of the decay envelope centroid. However, Fig. 8 demonstrates that, for the Sim-2 model, the existence of noise has a positive effect. Noise will appear in the steady-state responses thus displacing the time centroid to the right and making the transient response

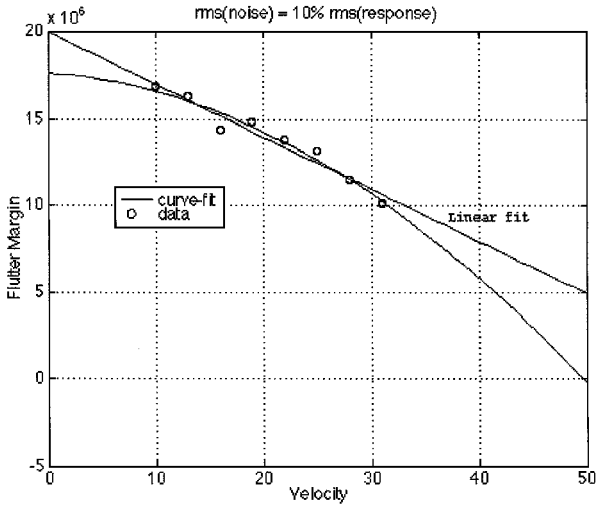

Fig. 6 Flutter margin variation with velocity, 10% rms noise, with linear fit, Hancock model.

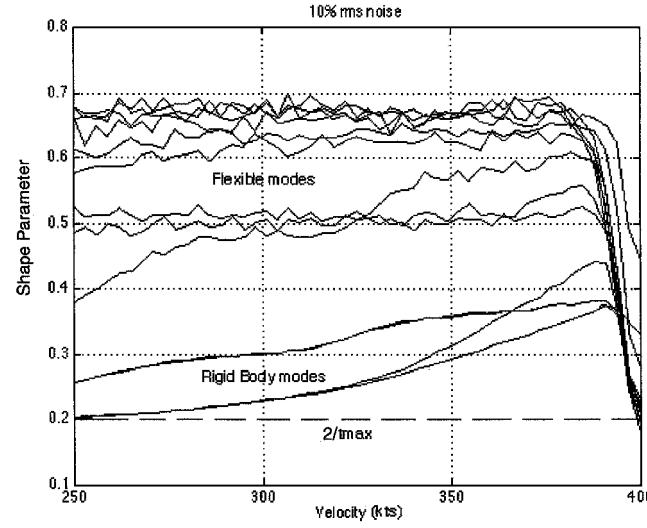

Fig. 8 Shape parameter variation with velocity, Sim-2 model, 10% rms noise.

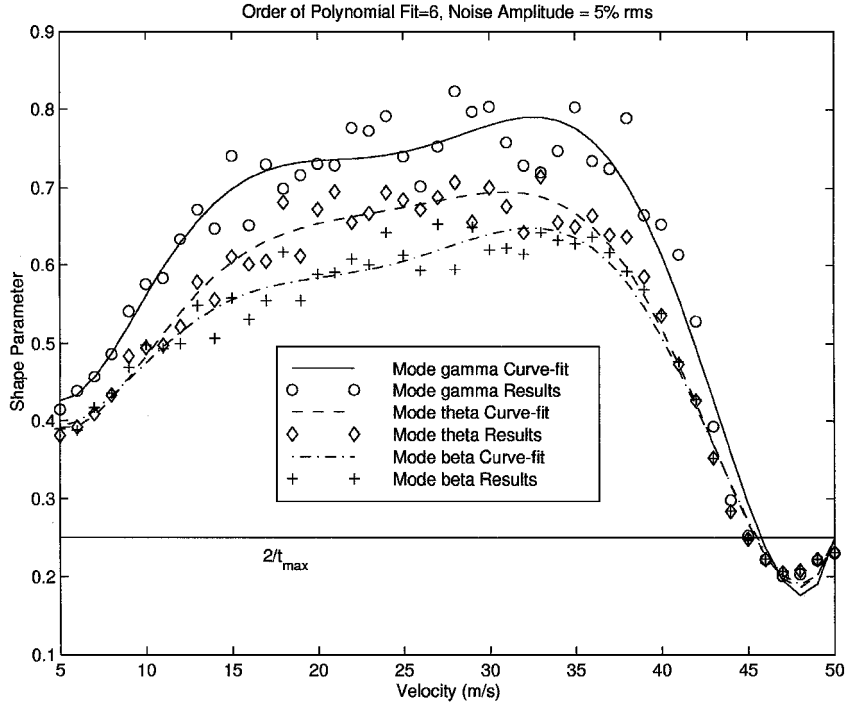

Fig. 7 Shape parameter centroid variation with velocity, Hancock model.

Table 3 Flutter speed estimates using envelope method, Hancock model

t_{max}	Best polynomial order	Best flutter speed estimates	% |Error|
		23–43 Range, %	
10	2	54.7619	24.2
8	2	49.7932	13.0
6	2	34.7932	21.1
		23–57 Range, %	
10	3	43.5895	1.1
8	3	43.1423	2.1
6	3	44.1552	0.2
		23–70 Range, %	
10	3	44.2338	0.4
8	3	44.3199	0.6
6	4	45.1514	2.4
		23–84 Range, %	
10	5	42.9772	2.5
8	5	46.1875	4.8
6	4	45.9741	4.3
		23–98 Range, %	
10	6	44.0838	0.0
8	4	44.0438	0.1
6	3	43.9444	0.3
		45–66 Range, %	
10	2	41.2831	6.3
8	2	41.0387	6.9
6	2	42.6185	3.3
		45–79 Range, %	
10	3	41.0289	6.9
8	3	43.2193	1.9
6	3	44.3230	0.6
		45–93 Range, %	
10	4	44.1043	0.1
8	4	44.1887	0.3
6	4	44.3050	0.5
		68–88 Range, %	
10	2	44.4217	0.8
8	2	44.2729	0.4
6	2	44.6352	1.3

less significant. Hence, apart from shape parameters obtained from measurement stations dominated by the rigid-body modes, the shape parameter variations in Fig. 8 are relatively flat at subcritical speeds. As flutter is approached, the transient response takes longer to decay and becomes more significant, resulting in a drop in the shape parameters. Hence, flutter is approached when the shape parameter trends are no longer flat. Thus, subcritical variations in the shape parameter can be ignored, making the detection of flutter a simpler process. Of course, at high noise levels, this advantage is lost because, the higher the noise amplitude, the more sudden the drop in the shape parameter near flutter.

As with the damping fit method, the appropriate order of the polynomial fit of the decay envelope centroid is far from obvious. The problem is that a single polynomial order can not be chosen to be adequate for a variety of test cases. Finally, the value of t_{max} does not appear to influence greatly the flutter predictions. Table 3 shows flutter predictions obtained by the envelope function method for the Hancock model. For each velocity range, three values of t_{max} are applied. None of these values appears to yield consistently more accurate predictions. Table 3 also shows the polynomial orders that yield the best flutter predictions for each test case.

NG

The NG modeling of the equations of motion of a system is very accurate for low-order models. The factors that affect the accuracy of the NG are the presence of noise and the velocities at which the subcritical tests take place. A further consideration is the number of air speeds at which tests are carried out. The NG only needs two tests at two different velocities to provide the complete equations of motion. However, during the course of the present research, the possibility that flutter predictions might improve if more than two velocities are used was examined. The basic premise of this idea is that if there are measurement errors in the responses used in the identification process then the identified equations of motion will also contain errors, resulting in less accurate flutter predictions. Hence, if tests are carried out at more than two velocities and the aerodynamic and structural matrices obtained by a least-squares procedure, the flutter estimates might improve.

Table 4 Flutter estimates by the NG method using different numbers of test speeds

Number of air speeds	Flutter speed estimate, m/s
2	44.0761 ± 0.0434
3	44.0931 ± 0.0600
4	44.1506 ± 0.0720
5	44.1208 ± 0.0656
6	44.0532 ± 0.0715
7	44.1218 ± 0.0564
8	44.1468 ± 0.0526

To test this idea, the Hancock model was used in the 10–30 m/s velocity range (or $0.23V_f$–$068V_f$). The first test was carried out with two velocities, one at 10 m/s and one at 30 m/s. The second test was carried out with three velocities, one at 10, one at 20, and one at 30 m/s. In all, seven tests were carried out with up to eight velocities, all within the same range. The responses in all of the tests were contaminated with 10% rms white noise, chosen from a normal distribution with zero mean and unity variance. Each test case was repeated 100 times to provide a large population of flutter speed estimates. The confidence bounds of the mean flutter estimate for each test case were calculated using the Student's T test[17] with a confidence level of 1%. The results are given in Table 4. It can be seen that the best result, both in terms of mean flutter speed and confidence bounds, occurs in the case where only two speeds are used. The conclusion drawn from these results is that there is no advantage in using more than two test speeds to identify a simple system such as the Hancock model with the NG method. A higher number of air speeds would only be required if the aerodynamic lag terms had not been neglected in the derivation of the method.

As the noise level increases, the quality of identification by the NG decreases, as can be seen in the left-hand side of Fig. 9. The Hancock model contains no structural damping so that the damping ratios should be zero at zero velocity, but the quality of identification in the presence of 10% rms noise is so low that the predicted dampings at zero velocity are nonzero. Additionally, parts of the identified frequency variation are inaccurate. The adverse effects of experimental errors can be overcome by using more than one forcing vector during identification. With four forcing vectors and with 20% rms noise, for the same test case, the quality of identification was much improved, as seen in the right-hand side of Fig. 9

The NG method was not applied successfully to the Sim-2 model. The large number of modes in the Sim-2 model, coupled with the fact that the equations of motion are stiff, that is, some of the system eigenvalues are orders of magnitude larger than the low-frequency eigenvalues, caused matrix T in Eq. (13) to be badly scaled and, hence, nearly singular. As a consequence, the resulting equations of motion were highly inaccurate.

ARMA-Based Method

The MA part of an ARMA model implies white noise excitation; however, because all of the other methods were evaluated using frequency sweep excitation signals, an autoregressive moving average with exogenous inputs (ARMAX) model was used instead of ARMA to ensure a fair comparison of the methods. Exogenous inputs refers to inputs other than white noise.

The first difficulty in the implementation of the method is the evaluation of the ARMAX coefficients. In the absence of noise, this evaluation can be accomplished quite successfully even using a simple least-squares procedure with J equal to the number of modes.

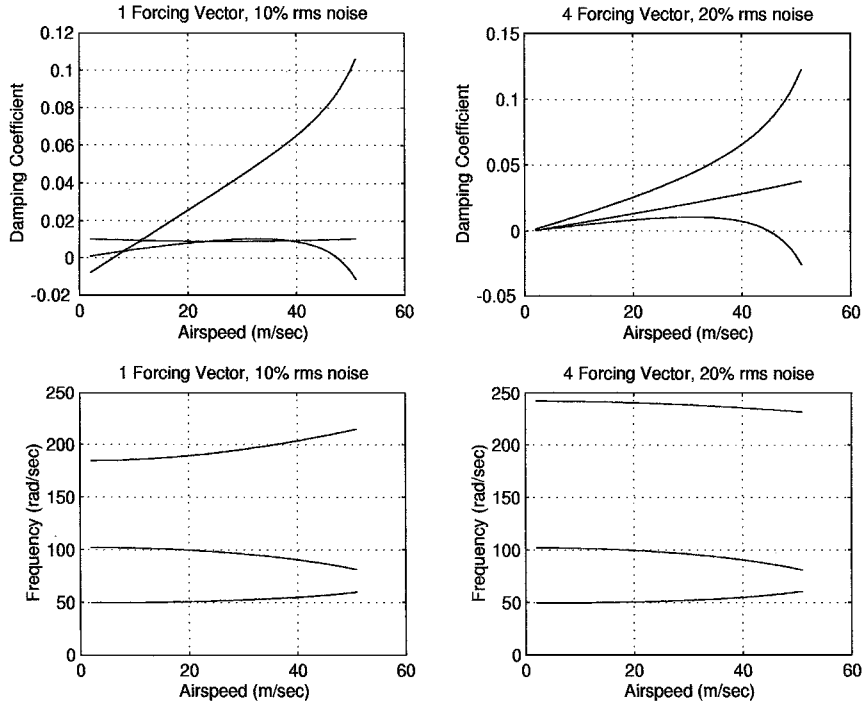

Fig. 9 Comparison of performance of NG with 1 and 4 forcing vectors.

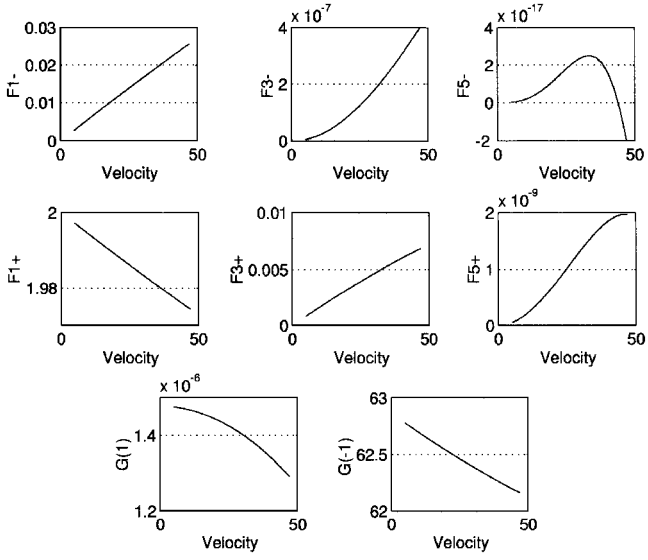

Fig. 10 *F* and *G* stability criteria using ARMA method, no noise, Hancock model.

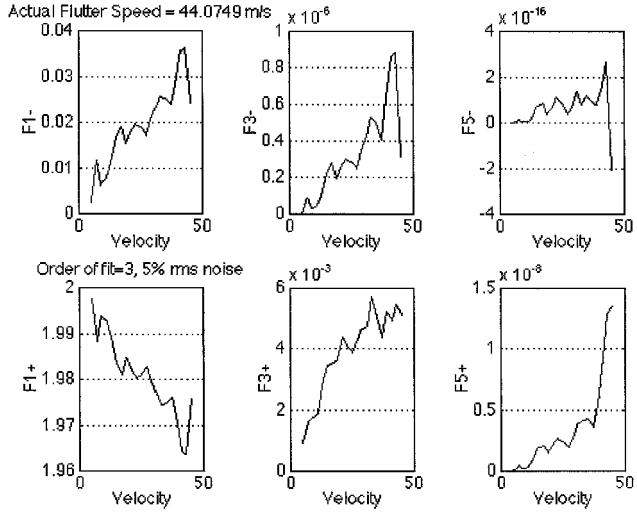

Fig. 11 *F* stability criteria using ARMA method, 5% noise, third-order model.

Then, the response of the ARMAX model to a given signal is almost identical to that of the actual system. In Fig. 10, all of the stability criteria are plotted for a range of velocities up to the flutter velocity for the Hancock noise-free case. Criterion F_5^- goes negative at an air speed very close to the actual flutter velocity. However, it can be seen that the drop in the value of F_5^- is very abrupt, giving the impression of hard flutter, even though Fig. 1 shows that the Hancock model does not undergo hard flutter. If a curve fit of the criterion was attempted at low subcritical speeds, it would fail to predict flutter. References 12 and 18 suggest a linear curve fit very close to the flutter velocity; however, such a procedure would carry considerable risks in the case of an experimental test, be it in the wind tunnel or in the air.

When the responses contain noise, the evaluation of an accurate ARMAX representation of an aeroelastic system becomes very difficult. A number of parameter estimation schemes were used in the application of the method to the Hancock wing with control surface model with 5% rms noise in the response. These included standard least squares, instrumental matrix with delayed observations, double least squares[14] and the recursive filtering method.[13] Figure 11 shows the estimated F stability criteria for a best-case application using double least squares and J equal to the number of modes. Despite the noise, F_5^- is correctly identified as the first criterion to go negative; however, the curves are obviously very rugged and would not admit a successful polynomial curve fit. The flutter velocity was identified accurately, but only after tests were performed at a high subcritical speed. For $J = 5$ (number of modes + 2), the resulting criteria are worse. The authors of Refs. 12 and 18 suggest a maximum likelihood approach for order determination and parameter estimation; however, they do not mention any applications of that approach to the case were there are measurement errors in the responses in either of these references.

The best results for the Hancock model were obtained when using J equal to the number of modes with double least squares. The

response results were decimated, that is, the time step was increased because when the time step is very small the curve fit is more sensitive to noise corruption.[14] Nevertheless, the ARMAX results in Table 1 are very disappointing, with only test cases very close to flutter yielding acceptable predictions.

For the Sim-2 model, the best ARMAX fits were obtained using normal least squares and J equal to the number of modes. It was found that small amounts of noise improved the fits. Figure 12 shows a typical fit of the response of transducer number 7 (located at the tip of the tailplane, midchord). The agreement between the ARMAX model and the Sim-2 results is very good. The performance of the ARMAX method is generally better for the Sim-2 model than for the Hancock model. This is because, due to the high number of modes, there are many more $F^{\pm}(l)$ stability criteria. Figure 13 shows the $F^{+}(l)$ criteria for a sample application [criteria $G(1)$ and $G(-1)$ do not go negative and the $F^{-}(l)$ criteria go negative after the $F^{+}(l)$ ones]. The critical criterion is $F^{+}(45)$ because it assumes negative values first. Hence, the flutter velocities in Table 2 were obtained by polynomial curve fits of $F^{+}(45)$.

Sensitivity of the Methods to Noise

An indication of the sensitivity of the methods to measurement noise was obtained by the application of the techniques to data

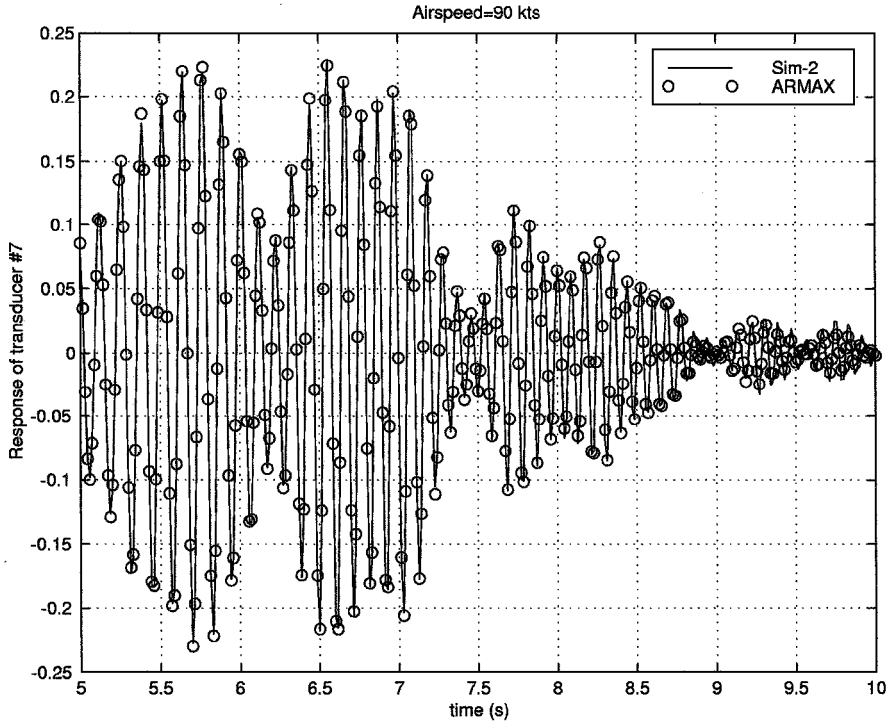

Fig. 12 Sample ARMAX fit of the Sim-2 model response to chirp input.

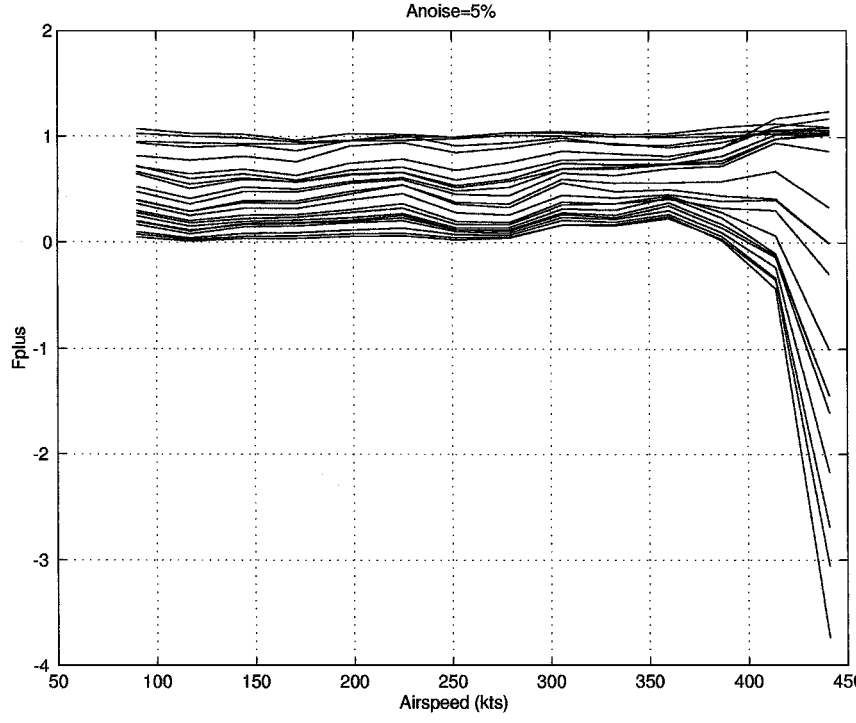

Fig. 13 $F^{+}(l)$ stability criteria variation with air speed for Sim-2 model.

Table 5 Variation of error in flutter estimates with increasing noise level, Hancock model

Noise	Damping fit		Envelope		NG		FM		ARMAX based	
% rms	Error, %	STD	Error, %	STD	Error, %	STD	Error, %	STD	Error, %	STD
5	3.1	1.1	−3.0	5.7	−0.1	0.2	2.4	0.7	7.4	19.9
10	−1.3	1.3	−9.6	8.1	−0.5	1.0	7.9	1.9	10.1	16.2
15	5.8	7.7	−15.8	14.2	−0.7	1.4	13.3	2.6	12.0	15.6
20	50.0	112.6	−26.8	13.8	1.8	4.9	29.9	8.1	20.8	19.9

from the Hancock model corrupted with simulated noise of increasing amplitude. The noise was white noise with a square frequency spectrum, incorporating frequencies up to twice the highest natural frequency of the system. The noise amplitude was measured as a percentage of the rms amplitude of the clean response. Tests were carried out with all of the methods at noise levels of 5, 10, 15, and 20% at an air speed range between 20 and 80% of the flutter speed. Each test was repeated 30 times, and the mean flutter predictions as well as their standard deviations (STDs) were calculated. The mean errors in the flutter predictions and STDs are given in Table 5.

The damping fit approach appears to perform well up to a noise amplitude of 15% (even though, at that amplitude, the spread of the results is quite high), but fails completely at 20% rms noise amplitude. The envelope function has a tendency to underestimate the flutter speed with increasing noise level. The NG approach (with four excitation vectors) is very robust, yielding very small errors and STDs even at noise levels of 20%. The FM yields unacceptable predictions at noise amplitudes higher than 10%. The performance of the ARMAX-based method is characterized by a very high spread of predictions, as witnessed by the high values of STDs. If an error of up to 10% in the flutter estimates is considered acceptable, then the maximum allowable noise levels for each method are damping fit, 15%; envelope method, 10%; NG, 20%; FM, 10%; and ARMAX-based, 5%.

Three observations must be made. First, the flight conditions at which the tests are performed affect the sensitivity of the methods to noise. If test were performed very close to the actual flutter condition, then the methods would have been far less sensitive to noise. Second, the sensitivity of the methods to noise also depend on the particular implementation. For example, the way in which the damping ratios and envelope function values are curve fitted and extrapolated contributes to noise sensitivity. Third, in real flight flutter tests, the measurement noise is not necessarily white, and there may also be systematic errors included in the responses. Hence, the conclusions drawn in this section are only indicative.

Simulated Flutter Test

Simulated flutter tests were performed for both models using all of the flutter prediction methods. The procedure for all approaches (apart from the NG technique) was as follows:

1) The response of each model was first obtained at a low subcritical speed, equal to 22.7% of the actual flutter speed. In the case of the Sim-2 model, the response also depends on the flight altitude, which was fixed at 5000 ft. The responses were analyzed to provide estimates for the damping ratios, flutter margin, envelope function shape parameter, and ARMA-based stability criteria.

2) The flight speed was increased by an increment equal to 7% of the actual flutter speed, and estimates of the four stability parameters mentioned in step 1 were obtained.

3) The flight speed was increased again by the same increment of the actual flutter speed and estimates of the four stability parameters were obtained. Each of the parameters was fitted with respect to flight speed by a second-degree polynomial, whose roots were subsequently obtained. Any roots that were complex, lower to the current flight speed, or occurred at points of positive curvature were ignored. The remaining roots provided the first estimates for the flutter speed, a maximum of one estimate for each stability parameter. Subsequently, checks were performed to ensure that the next flight speed would not be within 20% of any of the flutter speed estimates. At this early stage in the testing procedure, all methods indicated stability for the next test point.

4) The flight speed kept being increased by the same increment, and new estimates for the stability parameters were obtained and added to the curve-fitting procedure. With each new estimate, higher orders of polynomial curve fits were possible. The flutter margin was only fitted by second-order polynomials, but the other three stability parameters were fitted by polynomials of all possible orders, with the new estimate for the flutter speed being calculated as the mean of all of the acceptable roots. After all of the new estimates were obtained, stability checks were performed for the next test speed.

5) The simulated flight test was ended at the test speed at which all methods predicted that the next test speed would be within 20% of the latest flutter speed estimates. For each of the methods, the final flutter speed estimate was taken to be the first estimate at which the stability check failed.

For the NG, the procedure was slightly different. At each test point, only the current and initial responses were used to provide a flutter estimate. Additionally, the NG was only applied to the Hancock model flutter tests.

All results were obtained for responses contaminated by 5% rms white noise. The noise was simulated by taking the inverse Fourier transform of a frequency signal with constant amplitude and random phase. The simulated flutter test procedure was repeated 30 times, and the mean flutter speed prediction and 5% confidence interval was calculated for each method.

Comparison Between Methods

From the discussion already presented, it should be clear that all of the flutter prediction methods investigated here can yield accurate predictions under certain circumstances. The crucial consideration that divides the techniques is how wide is this set of circumstances for each one of them. A further consideration is the ease of use and the speed of the calculations involved. During a flight flutter test, it is often very important to know as soon as possible whether proceeding to the next test point is safe.

The methods can be separated into two categories:

1) The first category consists of methods that identify the equations of motion. This category contains only the NG method, which requires the DOF or modal responses. The identification requires only two tests at two different velocities. The equations of motion can then be solved to yield the flutter speed.

2) The second category consists of methods that curve fit a stability criterion. This category contains the rest of the methods (damping fit, FM, envelope, and ARMA). They all calculate a parameter that characterizes the stability of a system at each test velocity. The parameter variation with air speed is curve fitted by a polynomial and then extrapolated to the condition for instability, to yield the flutter velocity.

The results of Tables 1 and 2 show that, as expected, the predictions from all of the methods tend to improve when the tests are performed near the actual flutter condition. For example, the predictions for the air speed range 23–98% (of the flutter speed) are never more than 0.5% out. However, this is only a general trend. In Table 1, for example, as the test speed range is widened, the damping fit prediction error falls from 14.4 to 5.1%, increases to 9.1%, and then falls again to 0.1%. Because, with the inclusion of noise, all of the processes are stochastic, there are always going to be glitches in the general trends. Nevertheless, the patterns that emerge show

Table 6 Flutter predictions for the Hancock model, simulated flutter test

Method	Mean flutter speed estimate, m/s	Mean error, %
Damping fit	43.73 ± 1.054	−0.8
Envelope	46.00 ± 1.093	4.4
FM	45.34 ± 0.251	2.9
ARMAX-based	24.50 ± 2.176	−44.4
NG	44.13 ± 0.142	0.1

Table 7 Flutter predictions for the SIM-2 model, simulated flutter test

Method	Mean flutter speed estimate, kn	Mean error, %
Damping Fit	394.15 ± 5.88	−1.0
Envelope	386.82 ± 2.47	−2.8
FM	432.82 ± 5.38	8.8
ARMAX	164.08 ± 9.87	−58.8

that, for the Hancock model, the highest errors are obtained with the ARMAX-based method and the lowest with the NG method, whereas, for the Sim-2 model, the highest errors are again obtained from the ARMAX-based method whereas the envelope function method yields the lowest errors.

Simulated flight flutter predictions from the methods are given in Tables 6 (Hancock model) and 7 (Sim-2 model). Two striking features of the results in Tables 6 and 7 are the poor performances of the ARMAX-based method for both models and the FM on the Sim-2 model. The reason for the failure of the ARMAX method is the inability to obtain accurate ARMAX coefficients in the presence of noise, as detailed in the section on preliminary validation of the ARMAX method. The FM overestimated the flutter speed of the Sim-2 model by 8.8% because the fake flutter margin variation dropped very abruptly near flutter, that is, did not supply adequately early warning of impending instability.

As far as the accuracy of prediction, the equation-of-motion-identification method is best, as indicated by the Hancock model results. The NG provides consistently high-quality predictions even when the subcritical tests are carried out at relatively low velocities and under high levels of noise. The accuracy of the method derives from a number of responses to different inputs at the same test speed being employed in the calculations.

On the other hand, it was found that the category 1 method could not be successfully applied to the Sim-2 model. Only category 2 methods could provide results for that model, the damping fit approach being the most successful, followed by the envelope method. However, category 2 methods require polynomial curve fitting and, except in the case of the FM, the order of the polynomial is unknown. One way of determining which order of polynomial is best is to obtain a preliminary value for the flutter velocity. This can be provided either by using a mathematical model of the system under consideration or from earlier wind-tunnel and flight flutter tests. Additionally, with the exception of the envelope method, category 2 methods are complementary, that is, they all require a knowledge of the eigenvalues of the system. Once these have been evaluated for a particular test case, flutter predictions can be obtained very quickly and inexpensively. Hence, the damping fit, FM, and ARMA methods could conceivably be applied simultaneously at each test case.

Note that the present research indicates that, for large systems, the damping fit method is the most effective. This method also happens to be the most widely used approach in practical flight flutter tests. In a purely academic sense, category 1 methods are preferable to the damping fit technique because they provide a fuller picture of the dynamics of a given system. Nevertheless, in more realistic applications, category 1 methods are confronted by a number of practical problems such as the choice of the number of modes, the need for modal responses, and associated numerical problems. The damping fit method does not suffer from any of these difficulties. Any aeroelastic system, no matter how complex, will yield damping data and will have zero damping at the flutter speed.

Table 8 Comparative computational costs

Method	Time, s	FLOPs
ARMA	103.9080	558,279,907
Damp	119.0050	580,848,971
FM	93.4040	420,815,792
Envelope	58.6300	111,513,021
NG	19.2780	16,367,706

A final note should be made on the ARMA-based method. Its performance in both the stand-alone tests and the simulated flutter tests was much poorer than the performance of any of the other methods. The Jury stability criteria, which are employed to pinpoint the flutter velocity, have a very indifferent low subcritical variation, that is, flat and noisy, as seen in Fig. 13. Only near flutter does the variation become significant. Hence, any polynomial curve fit that uses low subcritical values of the stability criteria will yield large errors. In essence, the present research into the ARMA-based method sheds doubts on the suitability of the Jury stability criteria for the analysis of flight flutter test data.

In terms of computational effort, the category 1 method requires more data, especially if multiple excitation vectors are used, but fewer test speeds than category 2 methods. As Table 8 shows, the category 1 method is less expensive than category 2 methods, mainly because of the smaller number of tests. The computational time and number of floating point operations (FLOPs) data were obtained for a speed range of 10–43 m/s for the Hancock model. Category 2 method tests took place every 3 m/s in that range (a total of 12 tests). The category 1 method was applied with four excitation vectors. Of course, these results should only be seen as indicators of comparative computational costs, not as absolute assessments of the computational efficiency of each method.

Conclusions

Five different flutter prediction methods were implemented, and their performance was evaluated on two simulated systems. The criteria used in this evaluation were the quality of predictions and method complexity. The NG was found consistently to provide the most reliable predictions for the simple Hancock model; however, it failed completely for the larger Sim-2 model. The FM can yield acceptable results when applied to an aeroelastic system whose flutter mechanism is known, but it requires flight tests to be carried out at relatively high subcritical air speeds in the presence of high levels of noise corruption. The damping fit and envelope function method were found to give the best results for the Sim-2 model. The ARMA-based method was found to suffer in the presence of measurement error, mainly because of the inaccuracy of the ARMA-fitting procedure. Overall, the results presented show that the simplest methods appear to be the more robust while giving good accuracy. The more complex methods need further development to become more universally effective. Nevertheless, it was found that there was no general application of the techniques investigated here that would work for every aeroelastic model. The method implementations had to be specifically adapted for each model.

References

[1] Cooper, J. E., "Parameter Estimation Methods for Flight Flutter Testing," CP-566, AGARD, May 1995.

[2] Géradin, M., and Rixen, D., *Mechanical Vibrations*, Wiley, 1997.

[3] Zimmerman, N. H., and Weissenburger, J. T., "Prediction of Flutter Onset Speed Based on Flight Testing at Subcritical Speeds," *Journal of Aircraft*, Vol. 1, No. 4, 1964, pp. 190–202.

[4] Price, S. J., and Lee, B. H. K., "Evaluation and Extension of the Flutter-Margin Method for Flight Flutter Prediction," *Journal of Aircraft*, Vol. 30, No. 3, 1993, pp. 395–402.

[5] Routh, E. J., *Advanced Part of a Treatise on the Dynamics of a System of Rigid Bodies*, 5th ed., Vol. 2, MacMillan, 1930.

[6] Dickinson, M., "CF-18 Flight Flutter Test (FFT) Techinques," CP-566, AGARD, May 1995.

[7]Cooper, J. E., Emmett, P. R., Wright, J. R., and Schofield, M. J., "Envelope Function: A Tool for Analyzing Flutter Data," *Journal of Aircraft*, Vol. 30, No. 5, 1993, pp. 785–790.

[8]Cooper, J. E., "Modal Parameter Identification Using Exponential Weighting," *Proceedings of the First International Conference on the Integration of Dynamics, Condition Monitoring and Control*, Manchester. A. A. Balkema Publishers, Rotterdam. 1999.

[9]Nissim, E., and Gilyard, G. B., "Method for Experimental Determination of Flutter Speed by Parameter Identification," AIAA Paper 89-1324, 1989.

[10]Gaukroger, D. R., Skingle, C. W., and Heron, K. H., "An Application of System Identification to Flutter Testing," *Journal of Sound and Vibration*, Vol. 72, No. 2, 1980, pp. 141–150.

[11]Eversman, W., and Tewari, A., "Consistent Rational-Function Approximation for Unsteady Aerodynamics," *Journal of Aircraft*, Vol. 28, No. 9, 1991, pp. 545–552.

[12]Matsuzaki, Y., and Ando, Y., "Estimation of Flutter Boundary from Random Responses Due to Turbulence at Subcritical Speeds," *Journal of Aircraft*, Vol. 18, No. 10, 1981, pp. 862–868.

[13]James, P. N., Souter, P., and Dixon, D. C., "A Comparison of Parameter Estimation Algorithms for Discrete Systems," *Chemical Engineering Science*, Vol. 29, 1974, pp. 539–547.

[14]Cooper, J. E., "Comparison of Some Time-Domain-System Identification Techniques Using Approximate Data Correlations," *Journal of Modal Analysis*, Vol. 4, No. 2, 1989, pp. 51–57.

[15]Dimitriadis, G., and Cooper, J. E., "A Method for Identification of Non-Linear Multi-Degree-of-Freedom Systems," *Proceedings of the Institute of Mechanical Engineers*, Pt. G, Vol. 212, 298, 1998, pp. 287–298.

[16]Bennett, R. M., "Application of Zimmerman Flutter-Margin Criterion to a Wind-Tunnel Model," NASA, TM 84545, 1982.

[17]Stroud, K. A., *Engineering Mathematics*, 2nd ed., MacMillan, New York, 1970.

[18]Matsuzaki, Y., and Torii, H., "Response Characteristics of a Two-Dimensional Wing Subjected to Turbulence Near the Flutter Boundary," *Journal of Sound and Vibration*, Vol. 136, No. 2, 1990, pp. 187–199.